Proceedings of The Institute of Acoustics

NEAR-WALL RESPONSE OF UNSTEADY TURBULENT FLOWS. PART I. FLUID DYNAMICS

R R Mankbadi (1),(2) and J T C Liu (1),(3)

(1) Brown University, USA (2) Cairo University, Egypt
(3) Imperial College of Science and Technology, UK

ABSTRACT

The near-wall response of periodically-forced turbulent flows is considered and we deal with the fluid dynamical and computational aspects of the problem in this paper. The corresponding, modulated turbulent Stokes layer problem is solved with extensions of the rapid distortion theory, precisely in the frequency range where quasi-steady assumptions would fail. The computed unsteady velocity oscillations and modulated turbulent stresses compare favorably with observations in the "non-quasi-steady" frequency ranges. This forms the basis for the acoustical acpects of the problem to be reported subsequently.

INTRODUCTION

Pulsating turbulent flow in pipes and channels and over flat plates has received special recent attention since it provides relatively simple configurations for fundamental studies of unsteady turbulent shear flows and their possible control through forcing. Karlsson [1] was the first to study pulsating turbulent boundary layers over a flat plate. Recently Binder & Kueny [2], Cousteix, et al. [3], Parikh, et al. [4] and Binder, et al. [5] studied experimentally pulsating flows in channels and Tu & Ramaprian and Shemer, et al. [7] addressed the pipe flow problem. A compilation of existing data on pulsating, wall-bounded turbulent flows can be found in Carr [8].

One general result from the experiments is that no preferred frequencies were found, in contrast to excited free turbulent flows. However, for wall-bounded flows the modifications of the turbulence structure by pulsations nevertheless do depend on the frequency range. At low frequencies, Carr [8] pointed out that a quasi-steady behavior is observed as would be expected. The time- or Reynolds-averaged mean velocity profile is practically the same as that for steady flow with the same local external flow. In this case, although there is significant variations in the turbulence energy and shear stress, their ratio remains at the quasi-steady value. As the imposed oscillation frequency is increased beyond a "critical" value, there appear significant interactions between the periodic oscillations and the turbulence structure. Mizushina, et al. [9] relates this critical frequency to the turbulent burst in the flow and sho that the intensity of turbulence no longer follows that observed in the unperturbed flow case. In the same post-critical frequency range Ramaprian, et al. [10] also observed that the turbulence structure near the wall is perturbed out of equilibrium. The appropriately phased-averaged turbulence intensities and shear stress experience rather large phase shifts which are frequency dependent.

Several attempts have recently been made at computing periodic turbulent shear flows at various levels of modelling effort [3],[6],[11]-[13]. The main defect being that closure relations were identical to that used for steady flows and thus have not been successful, except in the the quasi-steady region, in the comparison with observations beyond the "critical" frequency region as pointed by Hanjalić & Stosić [12]. Furthermore, in these models the near-wall velocity was taken to be that given by the law of the wall for steady flows. Thus the important issue of the turbulent Stokes layer was completely circumvented. More recently, Kebede, et al. [14], using the full Reynolds stress model but with quasi-steady closure, computed periodic turbulent flow properties down into the viscous layer region. For application to pulsating turbulent flows, however, the results were time-step dependent and deviated considerably from observations. On the basis of their observations, Binder & Kueny [2] point out the relevant length scale of the near-wall region being that of the viscous Stokes layer $\sqrt{\nu/\omega}$ to that of the near-wall viscous layer in turbulent shear flow ν/U_*, where ν is the kinematic viscosity, ω the forcing frequency and U_* the frictional velocity. In fact, the "critical" frequency is in the vicinity when the ratio of the two layers is of order unity, that is, when the parameter $l_s^+=\sqrt{2U_*^2/\nu\omega}$ is of the order of ten. In this parameter region the dynamical effects of the periodic forcing strongly influences the wall-region viscous layer of the turbulent shear flow. In fact Cousteix [15] concluded that the correct description of the near-wall region would be essential towards obtaining the wall shear stresses at the intermediate and high frequency regions. The socalled "critical" frequency region is now understood interms of the parameter l_s^+ being of order ten or thereabouts.

In the present paper we focus our attention on an appropriate, but simplified, modelling of pulsating turbulent flows at the "high frequency" region interms of the parameter l_s^+ where quasi-steady models have been known to be inadequate. The theoretical consideration naturally follows the feasability indicated by experiments [16],[17] in separating the time-dependent, phase-averaged field from the time-independent Reynolds-averaged field. In fact, Carr's [8] survey indicate that experimentally the mean field is not affected by the pulsations and can infact be obtained from quasi-steady models which we shall regard as being given here. For the near-wall phased-averaged field, we shall solve the momentum equation for the periodic velocity component in conjunction with the phase-averaged turbulent kinetic energy equation supplemented with relations obtained from extensions of the rapid distortation theory (e.g. Maxey [18]).

FORMULATION

The physical problem concerns the near-wall response of periodically forced channel, pipe or turbulent boundary layer flow. To fix ideas consider the flat plate problem with an external velocity of the form

$$U_0(t)=\overline{U}_0+A\exp(i\omega t), \tag{1}$$

where t is the time, $\overline{U}_0$ is the time-averaged external velocity and A is the amplitude of the imposed pulsation. In the external region the oscillating velocity is equivalent to the oscillations in the pressure gradient given by an inviscid relation

$$\tilde{p}_x=-i\omega A\exp(i\omega t), \tag{2}$$

where $\tilde{p}$ is the oscillating pressure (with the fluid density absorbed into its denominator for convenience), x is the streamwise coordinate. Differentiations are indicated by subscripts. Correspondingly, the derivation of the fundamental equations for the mean motion, periodic component and turbulence follows from the splitting of the total flow quantity $Q(x_i,t)$ into the three components

$$Q(x_i,t)=\overline{Q}(x_i)+\tilde{q}(x_i,t)+q'(x_i,t), \tag{3}$$

where $\overline{Q}$ is the time averaged component, $\tilde{q}$ the period component and q' denotes the turbulence. The derivation of the appropriate conservation equations is now fairly standard, even for multiply-interacting periodic modes (see, e.g., Liu [19]), it suffices only to briefly outline the procedure and state the results at the simplified level. The time average, denoted by $\overline{(\ )}$, is supplemented by the phase average denoted by $<(\ )>$. If we substitute the decomposition into the full Navier-Stokes equations for an incompressible fluid, the mean flow momentum equations are obtained by time averaging. If we subtract the mean flow equations from the phase-averaged ones the momentum equations of the periodic component $\tilde{q}$ would be obtained. The crucial link with the turbulence comes from the modulated turbulent stresses denoted by

$$\tilde{r}_{ij}=<u_i'u_j'>-\overline{u_i'u_j'} \ , \tag{4}$$

where u_i' denotes the turbulent velocity components.
The momentum equations for the turbulence is then obtained by subtracting the phase-averaged momentum equations from those for the total flow quantity. The definition of the modulated stresses $\tilde{r}_{ij}$ above gives the clue for their derivation; the modulated kinetic energy, denoted by $\tilde{R}$, is but a special case of $\tilde{r}_{ij}$ or it can be obtained in a direct manner. The equations so obtained are stated in [19] and in the following we shall deal with the limited versions, through appropriate arguments, for the physical problem at hand.

<u>Simplifications</u>
The extent of the near wall region normal to the surface is "thin" relative to the streamwise extent and all x-derivatives (except for the external pressure) are neglected relative to the derivatives normal to the wall. The pressure is constant across the near-wall region. The vertical velocity is absent and the flow is unidirectional and thus $\tilde{u}=\tilde{u}(y,t)$ where y is the coordinate normal to te wall. The problem is further simplified by considering small perturbations and a linear description suffices.
Even is this much simplified framework, $\tilde{u}$ is coupled to the modulated and mean turbulent flow field through the action of the modulated stress in the $\tilde{u}$ momentum equation, $\tilde{r}_{xy}$. Rather than to deal with transport equations for the shear andnormal stresses, we choose to include only the modulated turbulent kinetic energy equation for $\tilde{R}$. This is motivated by the earlier work of Bradshaw, et al. [20] for the mean flow problem. In this case, there is no explicit need to make closure statements about the elusive pressure-velocity strain correlations since for the energy equation the action of the presurre gradients is recast into the "diffusional" effect due to pressure work. Even with nonlinear effects included, the diffusional effects include additionally the turbulent transport of $\tilde{R}$. This, together with the transport dur to pressure work can be neglected in the near-wall region in favor of viscous diffusion alone.
The simplified momentum equation for the periodic flow and for the modulated turbulent energy are then

$$\frac{\partial\tilde{u}}{\partial t}=-\frac{\partial\tilde{p}}{\partial x}+\nu\frac{\partial^2\tilde{u}}{\partial y^2}-\frac{\partial\tilde{r}_{xy}}{\partial y} \ , \tag{5}$$

$$\frac{\partial\tilde{R}}{\partial t}=-\tilde{r}_{xy}\frac{d\overline{U}}{dy}-\overline{R}_{xy}\frac{\partial\tilde{u}}{\partial y}+\nu\frac{\partial^2\tilde{R}}{\partial y^2}-\tilde{\varepsilon} \ , \tag{6}$$

where $-\bar{R}_{xy}$ is the mean Reynolds shear stress which, together with the mean velocity U, are considered as given functions of y. The problem requires the closure relation for the modulated viscous dissipation rate $\tilde{\varepsilon}$ and the relation between $\tilde{r}_{xy}$ and $\tilde{R}$. The boundary conditions require the no-slip condition at the wall and that $\tilde{u}$ and $\tilde{R}$ approach some limit "far" away from the wall. We shall state the boundary conditions after appropriate scaling, following closure arguments.

Closure Arguments. Extensions of Rapid Distortion Ideas
We refer to Hunt [21] for a review of rapid distortion theory and some of its applications and to Maxey [18] for a re-examination of the theory with respect to description of channel and pipe flows. The main formal assumption is that the fluctuating strain rates of the relatively large eddies are much weaker than the distortion due to the mean shear. For the perturbed, "high" frequency turbulent shear flows it is concievable that distortions would take place over timescales short compared with the timescales for the decay of the relatively large eddies. In this situation, rapid distortion theory could be justified for applications to the frequency range of practical interest.
On the other hand, for unperturbed turbulent shear flows, where the basic assumption of rapid distortion is not entirely satisfied, Townsend [22]-[23], nevertheless has shown that the turbulence structure can be satisfactorily described. Although rapid distortion theory does not provide the practical framework for a turbulence model, it nevertheless provide the ratio of the stresses to the turbulent kinetic energy interms of an effective distortion strain. The quantitative formulation for the effective distortion strain [18] then provides the remaining closing relation between the stresses and energy. The extensions of these ideas to periodically-perturbed turbulent shear flows are described in the following.
On the basis of an initial axisymmetric spectrum tensor, rather than isotropic, Maxey [18] computed velocity moments from the rapid distortion theory relating the general two-point velocity to such a tensor. The result for the ratio of the shear stress to the energy appears in the form

$$R_{xy}=F(\alpha)K, \tag{7}$$

where R_{xy} is the shear stress, K the energy and α is taken to be the effective strain for a locally uniform shear. The function $F(\alpha)$ for small strains is of the form

$$F(\alpha)=a\alpha/(1+b\alpha^2), \tag{8}$$

where $a=(2/5)[(3/S)-1]/[1+(2/S)]$ and $b=(1/35)[(21/S)-15]/[1+(2/S)]$. The initial anisotropy ratio S for shear flows is defined as the ratio of twice the largest normal stress (the streamwise component) to the sum of the two remaining normal stresses, evaluated at the centerline for pipe and channel flows. Maxey [18] showed that existing experiments give S of about 1.8 for channel flows and 1.2 for pipe flows. For initially isotropic turbulence S=1 and the maximum of the stress ratio $F(\alpha)$ is about 0.74 and this is reduced to about 0.42 when S=2
For locally uniform shear, a relaxation equation describing α was proposed by Maxey [18], which, in the present context, take the form

$$\partial\alpha/\partial t=\partial U/\partial y-\alpha/T \tag{9}$$

where T is an eddy timescale. The advantage of (9) is that it recovers the limit of equilibrium flow for long timescales, in which case $\bar{\alpha}=Td\bar{U}/dy$; and for small timescales the rapid distortion form is obtained, $\partial\alpha/\partial t=\partial U/\partial y$. Clearly, proposals for turbulent diffusion of the effective strain [22] and the viscous diffusion in the near-wall region, require further careful study. Here, we regard (9) as basic to our study.
The imposed periodicity upon an existing steady external velocity, given by (1) then suggests the perturbation of (7)-(9), consistent with (5) and (6), in the following form

$$R_{xy}=\bar{R}_{xy}+\tilde{r}_{xy},\ K=\bar{K}+\tilde{k},\ F(\alpha)=F(\bar{\alpha})+\tilde{\alpha}F'(\bar{\alpha}),\ \alpha=\bar{\alpha}+\tilde{\alpha},\ U=\bar{U}+\tilde{u}. \tag{10}$$

Substitution of (10) into (7)-(9), the small perturbation relations obtained are then

$$\tilde{r}_{xy}=F(\bar{\alpha})\tilde{k}+F'(\bar{\alpha})\bar{K}\tilde{\alpha}\ , \tag{11}$$

$$\frac{\partial\tilde{\alpha}}{\partial t}=\frac{\partial\tilde{u}}{\partial y}-\frac{\tilde{\alpha}}{T}\ . \tag{12}$$

Relations (11) and (12) will enable us to replace $\tilde{r}_{xy}$ by $\tilde{k}$ in (5) and (6). The final closure argument is with regard to the modulated viscous dissipation rate $\tilde{\epsilon}$. We rely on the argument that the smaller eddies contribute to viscous dissipation and their timescales are such that they are nearly in equilibrium. In this case, $\tilde{\epsilon}$ would be a perturbation from the usual postulated form [25]. For the present problem, we shall deduce the form for $\tilde{\epsilon}$ directly from the perturbation energy equation (6). The argument for the smaller eddies is that ter is a local equilibrium between production, given by the first two term on the right of (6), and dissipation in the wall region. If we further hypothesize for purposes of estimating $\tilde{\epsilon}$ that an eddy viscosity relation might hold for both the mean and modulated stresses, and if the eddy viscosities are the same then the two production terms are equal and are equated to the dissipation rate $\tilde{\epsilon}=2\tilde{r}_{xy}d\bar{U}/dy$. Because of the local equilibrium arguments, the quasi-steady form of the relation between the stress and energy is used, leading finally to

$$\tilde{\epsilon}=2F(\bar{\alpha})\frac{d\bar{U}}{dy}\tilde{k}\ . \tag{13}$$

The system (5),(6) and (11)-(13) then form the close set of equations for this study.

<u>The Boundary Value Problem: The Turbulent Stokes Layer</u>
Subject to the driving external flow of the form (1), the perturbation flow quantities are also assumed to be harmonic and may be represented by the real part of

$$\tilde{q}(y,t)=\hat{q}(y)\exp(i\omega t)\ , \tag{14}$$

where the amplitude functions $\hat{q}(y)$ are complex. After substituting flow quanti- of the form (14) into the system (5),(6) and (11)-(13), we further define non-dimensional quantities $U^+=\bar{U}/U_*$, $R^+_{xy}=\bar{R}_{xy}/U_*^2$, $u^+=\hat{u}/A$, $K^+=\hat{k}/AU_*$, $r^+_{xy}=\hat{r}_{xy}/AU_*$, and $\omega^+=\omega\nu/U_*^2$, $\epsilon^+=\hat{\epsilon}\nu/AU_*^3$, $y^+=yU_*/\nu$. We recall that A is the amplitude of the periodic part of the external velocity and that U_0 its steady part. In applications to pipe or channel flow problems, these will be regarded as the centerline values. The dimensionless form of (5) and (6) then appear as

$$i\omega^+u^+=i\omega^++u^{+\prime\prime}-r^{+\prime}_{xy} \quad (15)$$

$$i\omega^+K^+=-r^+_{xy}U^{+\prime}-R^+_{xy}u^{+\prime}+K^{+\prime\prime}-\varepsilon^+ \quad (16)$$

where a prime is used to denote differentiation with respect to y^+. The boundary conditions are

$$y^+=0: \quad u^+=K^+=0,$$
$$y^+\to\infty: \quad u^{+\prime}=K^{+\prime}=0. \quad (17)$$

The closure relations (11)-(13) becomes

$$r^+_{xy}= F(\bar{\alpha})K^++(d\ln F/d\bar{\alpha})R^+_{xy}\hat{\alpha} \quad (18)$$

$$\hat{\alpha}=A^+T^+u^{+\prime}/(1+i\omega^+T^+) \quad (19)$$

$$\varepsilon^+=2F(\bar{\alpha})U^{+\prime}K^+ \quad (20)$$

where $A^+=A/U_*$. The distortion timescale T^+ is estimated [18] to be about 3.5.

The Numerical Problem

The system of equations (15),(16) and (18)-(20) and the boundary conditions (17) form a boundary value problem. The variable coefficients, such as $R^+_{xy}, U^{+\prime}$ are obtained from experimental data in the wall region (e.g., [26]-[30]) and fitted with simple functions of y^+.

The boundary value problem was then solved using SUPPORT Programme [31]. The method of solution uses superposition coupled with an orthonormalization proceure and a variable-step Runge-Kutta-Fehlberg integration scheme. Each time the superposition solutions begin to lose their numerical linear independence, the vectors are reorthonormalized before integration proceeds. The basic principle of the algorithm is then to piece together the intermediate orthogonalized solutions, defined on the various subintervals, to obtain the desired solutions.

RESULTS AND DISCUSSION

We have previously defined the parameter l^+_s, which is essentially the ratio of the Stokes layer thickness $\sqrt{(2\nu/\omega)}$, to the near-wall region viscous length scale ν/U_*. Now l^+_s is related to the dimensionless frequency ω^+ as $l^+_s=\sqrt{(2/\omega^+)}$. when the viscous Stokes layer becomes of the same order as the wall region viscous layer, $l^+_s\approx 10$, in which case $\omega^+\approx 0.02$. This is the region where strong unsteady interactions in the near-wall region take place.

The calculated oscillations in the streamwise velocity is compared with the exerimental data of Binder & Kueny [2] in Figure 1. Their forcing was at low amplitudes. As would be expected, the results would be independent of such amplitudes. Figure 1(a) is for the case of $l^+_s=5.6$ ($\omega^+=0.0637$) and Figure 1(b) for $l^+_s=17$ ($\omega^+=0.0069$). In the higher frequency case an amplitude overshoot occurs, as would be expected of Stokeslike viscous layers, and this overshoot would move towards the wall as the frequency is increased. For the lower frequency case the amplitude overshoot near the wall is not at all obvious. In general he calculated amplitudes agree reasonably well with the data. The phase angle, rlative to that of the imposed velocity oscillations, compares well with the data for the higher frequency case. As in the large-amplitude forcing data [5], the phase shift near the wall is positive and approaches the Stokes value $\pi/4$. In the lower frequency case data [2],[5] the phase shift near the wall could become negative but in general, the phase shifts are not as spectacular as the higher frequency cases.

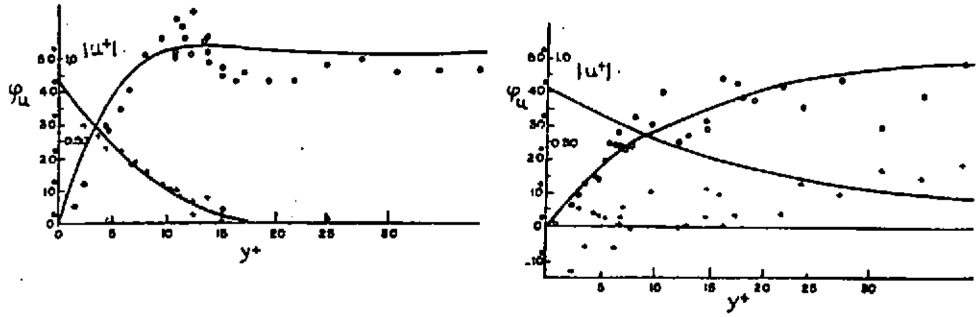

Figure 1. Comparison between computed oscillations in the streamwise velocity and measurements of Binder & Kueny [2], interms is the magnitude of u^+ and phase angle φ_u relative to their respective imposed values. (a) $\omega^+ = 0.0637$, (b) $\omega^+ = 0.0069$.

The oscillating wall shear stress is shown in Figure 2, in comparison with the measurements of Binder, et al. [5]. The magnitude, normalized by the Stokes value at the same frequency, is given in Figure 2(a): The phase angle φ_T, is referenced to the phase of the free stream velocity, is shown in Figure 2(b). Although the present theory is concerned with the relatively "high" frequency region of $l_s^+ \approx 10$ ($\omega^+ \approx 0.02$), the results are nevertheless shown for the extended region to $l_s^+ \approx 70$ ($\omega^+ \approx 0.0004$), covering the low frequency, quasi-steady region. The region of validity of the present theory can thus be examined. As expected, Figure 1(a) shows that the computed amplitude of the wall shear stress is in good agreement with the data in the region l_s^+ less than about 20 ($\omega^+ < 0.005$). At these "high" frequencies, the wall shear stress amplitudes dip below the Stokes value as in the experiments. This behavior has also been observed by Parikh, et al. [4]. At larger values of l_s^+ the wall shear stress magnitude is underestimated relative to observations. The computed phase shift in Figure 2(b)also agrees favorably with data for $l_s^+ < 15$ ($\omega^+ > 0.0089$). In the low frequency range the the phase angle is overestimated.

The computed wall shear stress is also compared with the data reported by Mao & Hanratty [32], in Figure 3. The magnitude of the oscillatory wall shear stress is normalized by the mean wall shear stress and by the dimensionless forcing velocity and is equivalent to the A defined previously. Figure 3(a) shows that the computed value is in good agreement with observations for $\omega^+ > 0.005$ as is expected. The phase angle in Figure 3(b) behaves qualitatively as observations in the frequency region $\omega^+>0.015$. It approaches the asymptotic value of about $\pi/4$. In the low frequency region, the phase angle is overestimated.

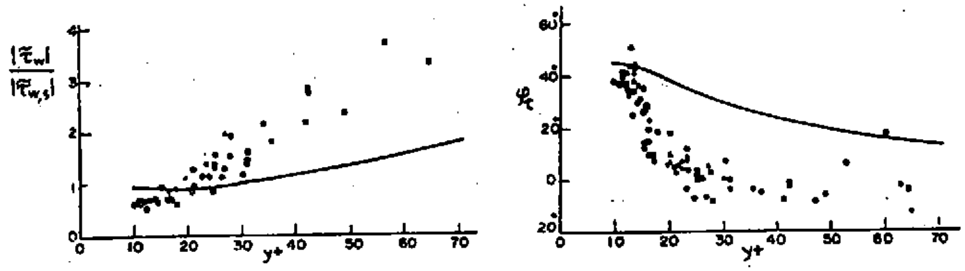

Figure 2. Oscillations of the wall shear stress compared with measurements of Binder, et al. [5], including forcing at large amplitudes: $A/\overline{U}_o$=0.10,●; 0.13,■; 0.17,▲; 0.19,○; 0.27,♦; 0.60,+; 0.70,□. (a) amplitude, (b) phase angle.

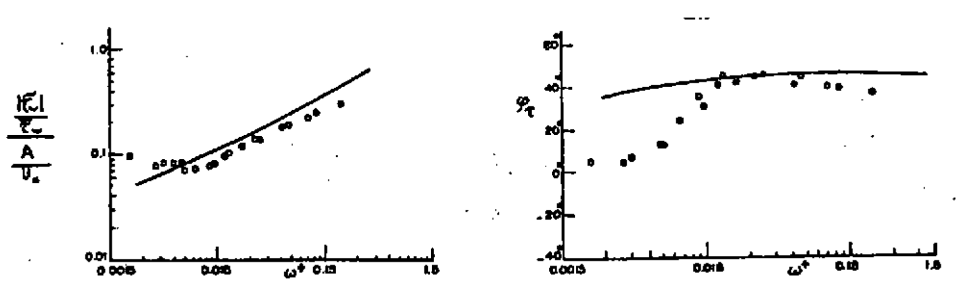

Figure 3. Oscillations of the wall shear stress compared with measurements of Mao & Hanratty [32]: ○, ● ; Ramaprian & Tu [33]: □ . (a) amplitude, (b) phase angle.

We recall the definition of the modulated turbulent normal stress due to the u-component of the turbulence fluctuations: $\tilde{r}_{xx}=\langle u'^2\rangle-\overline{u'^2}$. This quantity is of interest here in that it has been measured by Binder, et al. [5]. The comparison between our computed results and data is given in Figure 4 for the two values of ω^+=0.03 and 0.0038. The main features of the experimentally obtained structure is obtained. The peak values of $\tilde{r}_{xx}$ and its y^+ location both decrease as ω^+ increases. Infact the location of the peak is actually well described by the theory. However, Figure 4 indicates that this component of the normal stress is underestimated by the theory. This might be due the overestimation of viscous dissipation rates near the wall. Although not shown, the computed phase angle indicates that $\tilde{r}_{xx}$ lags behind $\tilde{u}$. This lag increases away from the wall and is increased as the frequency increases. And, in accordance with observations (e.g., [2],[5],[10]), it is clearly demonstrated that the modulated turbulence structure cannot be associated simply with the oscillating velocity.

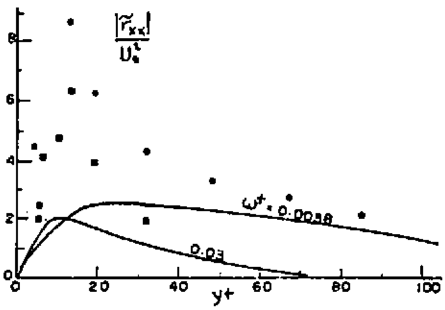

Figure 4. Modulated turbulent normal stress $\tilde{r}_{xx}/U_*^2$ compared with measurements of Binder, et al. [5]. $\omega^+=0.03$ ■, $\omega^+=0.0038$ ●.

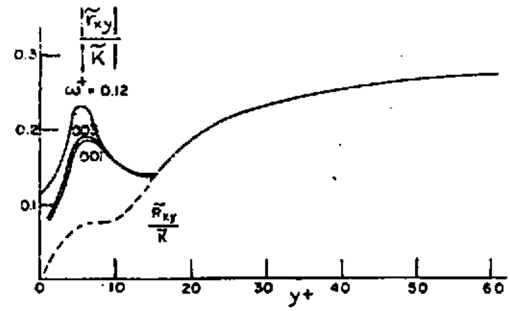

Figure 5. Ratio of modulated turbulent shear stress to kinetic energy.

The modulated turbulent shear stress, which is not shown here, has a peak in in the amplitude for a given frequency. As the frequency is increased, the peak decreases and moves closer to the wall. In contrast to $\tilde{u}'$, the shear stress varies considerably less with y^+. Thus no local relationship between the two uantities can be established in the near-wall region. In order to examine the departure of the modulated flow from structural equilibrium, we examine the ratio of the modulated shear stress to modulated turbulence energy. For equilibrium flows this ratio should be the same as that for steady flows. The amplitude of this ratio is shown in Figure 5. It is clear that the departure from equilibrium increases with frequency and reaches a maximum near the wall ($3<y^+<8$). For $y^+>20$ the modulated flow behaves like a quasi-steady one. This is onsistent with the structure of oscillating turbulent boundary layers [10]. The results also show that the phase angle of the modulated shear stress leads that of the energy and that this lead increases with frequency. The maxima of the phase lead occurs near the wall and decreases rapidly away.
This concludes our much abreviated description of the fluid dynamics of the near-wall response of periodically forced turbulent flows. On the one hand, the comparison with observation is sufficiently encouraging that it seems worthwhle to develop ideas from rapid distortion theory further for use in the description of a class of unsteady turbulent shear flows, including the fascinating problems involving coherent structures and their control [19]. On the other hand, the work described in this paper forms the basis for a full discussion of he acoustical aspects and implications [34], which will form Part II of this series to be reported subsequently.

This work is supported in part by DARPA/ACMP through its University Research Initiative, by NSF/FDHP Grant MSM-8320307, by NASA/Langley Research Center Grant NAG 3-673 and is also partially supported by NATO Research Grant 343/85, NSF U.S.-China Cooperative Research Program Grant INT-8514196 and by the U.K. SERC through its Visiting Fellow Program. This research is part of the activities of the Division of Engineering and the Laboratory for Fluid Mechanics, Turbulence and Computation at Brown University. The hospitality of the Department of Mathematics, Imperial College and that of J. T. Stuart, FRS to one of us (JTCL) is gratefully acknowledged. Although the responsibilities of this work rest with the authors, we are indebted to P. Bradshaw, FRS, M. R. Maxey and J. T. Stuart, FRS for the numerous helpful conversations.

REFERENCES

[1] Karlsson, S.K.F. 1959 J. Fluid Mech. 5, 622-636.
[2] Binder, G. & Kueny, J.L. 1981 In Unsteady Turbulent Shear Flows (R. Michel, et al., eds.), pp. 100-109. Springer-Verlag, Berlin.
[3] Cousteix, J., Houdeville, R. & Javelle, J. 1981 In Unsteady Turbulent Shear Flows (R. Michel, et al., eds.), pp. 120-144. Springer-Verlag, Berlin.
[4] Parikh, P.G., Reynolds, W.C. & Jayaraman, R. 1982 A.I.A.A. J. 20, 769-775.
[5] Binder, G., Tardu, S., Blackwelder, R.F. & Kueny, J.L. 1985 Symp. Turbulent Shear Flows 5, 16.1-16.8.
[6] Tu, S.W. & Ramaprian, B.R. 1983 J. Fluid Mech. 137, 31-58.
[7] Shemer, L. & Wygnanski, I. 1981 Symp. Turbulent Shear Flows 3, 8.13-8.18.
[8] Carr, L.W. 1981 In Unsteady Turbulent Shear Flows (R. Michel, et al., eds.), pp. 3-35. Springer-Verlag, Berlin.
[9] Mizushina, T., Maruyama, T. & Shiozaki, Y. 1973 J. Chem. Eng. Japan 6, 487-494.
[10] Ramaprian, B.R., Tu, S.W. & Menedez, A.N. 1983 Symp. Turbulent Shear Flows 4, 301-310.
[11] Menedez, A.N. & Ramaprian, B.R. 1983 U. Iowa Inst. Hydraul. Res. Rep. 270.
[12] Hanjalić, K. & Stosić 1983 Symp. Turbulent Shear Flows 4, 287-300.
[13] Cook, W.J., Murphy, J.D. & Owen, F.K. 1985 Symp. Turbulent Shear Flows 5, 18.3-18.18.
[14] Kebde, W., Launder, B.E. & Younis, B.A. 1985 Symp. Turbulent Shear Flows 5, 16.23-16.29.
[15] Cousteix, J. 1986 Ann. Rev. Fluid Mech. 18, 173-196.
[16] Shemer, L & Kit, E. 1984 Phys. Fluids 27, 72-76.
[17] Gibson, M.M. 1985 Symp. Turbulent Shear Flows 4, 219-222.
[18] Maxey, M.R. 1982 J. Fluid Mech. 124, 261-282.
[19] Liu, J.T.C. 1988 Adv. Appl. Mech. 26, 183-305.
[20] Bradshaw, P., Ferriss, D.H. & Atwell, N.P. 1967 J. Fluid Mech. 28, 593-616.
[21] Hunt, J.C.R. 1978 Fluid Dyn. Trans. 9, 121-152.
[22] Townsend, A.A. 1970 J. Fluid Mech. 41, 13-46.
[23] Townsend, A.A. 1976 The Structure of Turbulent Shear Flow (2nd ed.), pp. 80-88, 105-129. Cambridge U. Press.
[24] Townsend, A.A. 1980 J. Fluid Mech. 93, 171-191.
[25] Alper, A. & Liu, J.T.C. 1978 Proc. R. Soc. Lond. A. 359, 497-523.
[26] Laufer, J. 1954 N.A.C.A. Rep. 1174.
[27] Schubauer, G.B. 1954 J. Appl. Phys. 25, 188-196.
[28] Derksen, R.W. & Azad, R.S. 1981 A.I.A.A. J. 19, 238-239.
[29] El-Telbany, M.M.M. & Reynolds, A.J. 1981 J. Fluid Mech. 111, 283-318.
[30] Patel, V.C., Rodi, W. & Scheurer, G. 1984 A.I.A.A. J. 21, 1308-1319.
[31] Scott, M.R. & Watts, H.A. 1975 Sandia Labs. Rep. SAND75-0198.
[32] Mao, Z-X. & Hanaratty, T.J. 1986 J. Fluid Mech. 170, 545-564.
[33] Ramaprian, B.R. & Tu, S.W. 1983 J. Fluid Mech. 137, 59-81.
[34] Quinn, M.C. & Liu, J.T.C. 1985 Bull. Am. Phy. Soc. 30, 1743.